MEG sensor patterns reflect perceptual but not categorical similarity of animate and inanimate objects

Daria Proklova[1], Daniel Kaiser[2], Marius V. Peelen[3]

[1]*The Brain and Mind Institute, The University of Western Ontario, London, ON N6A 5B7, Canada*

[2]*Department of Education and Psychology, Freie Universität Berlin, 14195 Berlin-Dahlem, Germany*

[3]*Donders Institute for Brain, Cognition, and Behaviour, Radboud University, 6525 HR Nijmegen, The Netherlands*

Corresponding author:

Marius V. Peelen

Donders Institute for Brain, Cognition, and Behaviour

Radboud University

Montessorilaan 3

6525 HR Nijmegen

The Netherlands

Email: m.peelen@donders.ru.nl

Acknowledgements: The research was supported by the Autonomous Province of Trento, Call "Grandi Progetti 2012", project "Characterizing and improving brain mechanisms of attention – ATTEND". This project has received funding from the European Research Council (ERC) under the European Union's Horizon 2020 research and innovation programme (grant agreement No 725970).

Abstract

High-level visual cortex shows a distinction between animate and inanimate objects, as revealed by fMRI. Recent studies have shown that object animacy can similarly be decoded from MEG sensor patterns. What object properties drive this decoding? Here, we disentangled the influence of perceptual and categorical properties by presenting perceptually matched objects that were easily recognizable as being animate or inanimate (e.g., snake and rope). In a series of behavioral experiments, three aspects of perceptual dissimilarity of these objects were quantified: overall dissimilarity, outline dissimilarity, and texture dissimilarity. Neural dissimilarity of MEG sensor patterns, collected in male and female human participants, was modeled using regression analysis, in which perceptual dissimilarity (taken from the behavioral experiments) and categorical dissimilarity served as predictors of neural dissimilarity. We found that perceptual dissimilarity was strongly reflected in MEG sensor patterns from 80 ms after stimulus onset, with separable contributions of outline and texture dissimilarity. Surprisingly, MEG patterns did not distinguish between animate and inanimate objects after controlling for perceptual dissimilarity. Nearly identical results were found in a second MEG experiment that required object recognition. These results indicate that MEG sensor patterns do not capture object animacy independently of perceptual differences between animate and inanimate objects. This is in contrast to results observed in fMRI using the same stimuli, task, and analysis approach, with fMRI showing a highly reliable categorical distinction in ventral temporal cortex even when controlling for perceptual dissimilarity. The discrepancy between MEG and fMRI precludes the straightforward integration of these imaging modalities.

Significance statement

Recent studies have shown that multivariate analysis of MEG sensor patterns allows for a detailed characterization of the time course of visual object processing, demonstrating that the neural representational space starts to become organized by object category (e.g., separating animate and inanimate objects) from around 150 ms after stimulus onset. It is unclear, however, whether this organization truly reflects a categorical distinction or whether it reflects uncontrolled differences in perceptual similarity (e.g., most animals have four legs). Here we find that MEG sensor patterns no longer distinguish between animate and inanimate objects when controlling for perceptual differences between objects (e.g., when comparing snake and rope). These results indicate that MEG sensor patterns are primarily sensitive to visual object properties.

Introduction

After their successful application in fMRI research, multivariate analysis methods have recently been applied to MEG and EEG data to gain insight into the temporal dynamics of visual and cognitive processing. A replicable finding in this rapidly growing literature is the finding that object category (e.g., animacy) can be reliably decoded from MEG sensor patterns, peaking around 150-250 ms after stimulus onset (for review, see Contini et al., 2017). Similar category distinctions have been observed in high-level visual cortex using fMRI (Kriegeskorte et al., 2008b). What are the object properties that drive this decoding; and are these the same in fMRI and MEG?

Animate objects differ from inanimate objects in terms of their characteristic shapes and other category-associated visual features. These feature differences are reflected in behavioral measures of perceptual similarity, such that within- and between-category perceptual similarity can be used to accurately predict the time it takes observers to categorize an object as animate or inanimate (Mohan and Arun, 2012). These perceptual differences likely contribute to MEG animacy decoding considering that object shape and perceptual similarity can be reliably decoded from MEG and EEG patterns (Isik et al., 2014; Coggan et al., 2016; Wardle et al., 2016). Furthermore, MEG animacy decoding strength is closely related, at the exemplar level, to categorization reaction time (Ritchie et al., 2015), likely reflecting the exemplar's perceptual typicality of the category it belongs to (Mohan and Arun, 2012). Together, these studies raise the possibility that MEG animacy decoding primarily reflects perceptual differences between animate and inanimate objects.

However, animate and inanimate objects also differ in other aspects. For example, animals are agents capable of moving by themselves, a property that we rapidly associate with animals even when these are viewed as static pictures. Additionally, we perceive (most) animals as entities with goals, intentions, beliefs, and desires. Finally, animate and inanimate objects invite different actions on the part of the observer. For example, while animals may be perceived as threatening, inanimate objects are usually objects we grasp and interact with, such as tools, food, musical instruments, or clothing. Previous fMRI studies have provided evidence that category selectivity in visual cortex is partly driven by the task or function associated with an object, in addition to the object's visual properties (Amedi et al., 2017; Peelen and Downing, 2017).

One way to dissociate between these accounts is to compare neural responses to animate and inanimate objects that are perceptually matched (e.g., snake and rope). Recent fMRI studies adopting this approach revealed that category-specific responses in parts of ventral temporal cortex are not fully reducible to perceptual differences (Macdonald and Culham, 2015; Bracci and Op de

Beeck, 2016; Bryan et al., 2016; Proklova et al., 2016). In the fMRI version of the current MEG study (Proklova et al., 2016), we found that activity in large parts of the visual cortex reflected the perceptual similarity of the objects, independent of object category. But importantly, the animacy distinction in ventral temporal cortex was preserved for objects that were closely matched in terms of perceptual similarity. If MEG activity in the 150-250 ms time window corresponds to category-selective fMRI activity in ventral temporal cortex, animacy decoding should be preserved in MEG as well.

In marked contrast to this prediction, we report here that the careful matching for perceptual similarity of objects completely abolished animacy decoding in MEG: while representational similarity in MEG sensor patterns strongly reflected perceptual similarity between the objects, as well as similarity in their outline and texture properties, it no longer reflected the categorical distinction between animate and inanimate objects.

Materials and Methods

Participants

Twenty-nine participants in total with normal or corrected-to-normal vision took part in two experiments, including 14 volunteers who participated in Experiment 1 (5 females, mean age = 25.6 years, SD = 4 years) and 15 volunteers who participated in Experiment 2 (8 females, mean age = 25.2 years, SD = 3.1 years). All participants provided informed consent and received monetary compensation for their participation. The experimental protocols were approved by the Ethical Committee of the University of Trento, Italy.

Stimuli

The stimulus set in both experiments was identical to the one used in an earlier fMRI study (Proklova et al., 2016) and consisted of 16 objects (8 animate and 8 inanimate) divided into 4 shape sets. Each shape set consisted of 2 animals and 2 inanimate objects that were matched for overall shape features (e.g. snake-rope). In addition, four versions of each stimulus were used, resulting in a total of 64 stimuli. In Experiment 1, one additional visual stimulus (a hammer, see Figure 1A) was used to serve as an oddball target. All stimuli were matched for luminance and contrast using the SHINE toolbox (Willenbockel et al., 2010).

Experiment 1: Procedure

Participants viewed the visual stimuli while sitting in the dimly lit magnetically shielded room. The stimuli were projected on a translucent screen located 150 cm from the participant. The stimuli were presented centrally on the uniformly gray background and approximately spanned a visual angle of 8 degrees. The stimulus presentation was controlled using the Psychophysics Toolbox (Brainard, 1997). Participants completed 12 experimental blocks, with each of the 64 stimuli appearing exactly twice in each block, in random order. In addition, 32 target trials were randomly distributed throughout the block, resulting in 160 trials in total per block. The stimuli were presented for 500 ms, followed by a variable inter-stimulus interval ranging from 1.5 s to 2 s in discrete 20 ms steps. Participants were instructed to maintain fixation and to press the response button and blink each time they saw a picture of a hammer. This oddball image appeared on average every 5 trials. Target trials were not analyzed.

Experiment 2: Procedure

The procedure was largely identical to Experiment 1, differing only in the participants' task. Instead of an oddball detection, participants were asked to perform a one-back task, pressing the response button whenever an image of the same object appeared on two consecutive trials (e.g. two snakes). Twelve repetition trials were inserted at random points within each block, resulting in 140 trials per block. Repetition trials were not analyzed.

MEG acquisition and preprocessing

Electrophysiological recordings were obtained using an Elekta Neuromag 306 MEG system (Elekta Neuromag systems, Helsinki, Finland) equipped with 204 gradiometers and 102 magnetometers. Signals were sampled continuously at 1000 Hz rate and band-pass filtered online between 0.1 and 330 Hz. The data were then preprocessed offline using MATLAB and the Fieldrip Toolbox (Oostenveld et al., 2011). Data from all runs were concatenated and trials were epoched from 100 ms before to 500 ms after stimulus onset (for one follow-up analysis, trials were epoched from 100 ms before to 800 ms after stimulus onset). Trials containing eye-blinks and other movement-related artifacts were discarded from further analysis based on visual inspection. The signal was baseline-corrected with respect to the pre-stimulus window and downsampled to 100 Hz to reduce the processing time and increase the signal-to-noise ratio (Grootswagers et al., 2017).

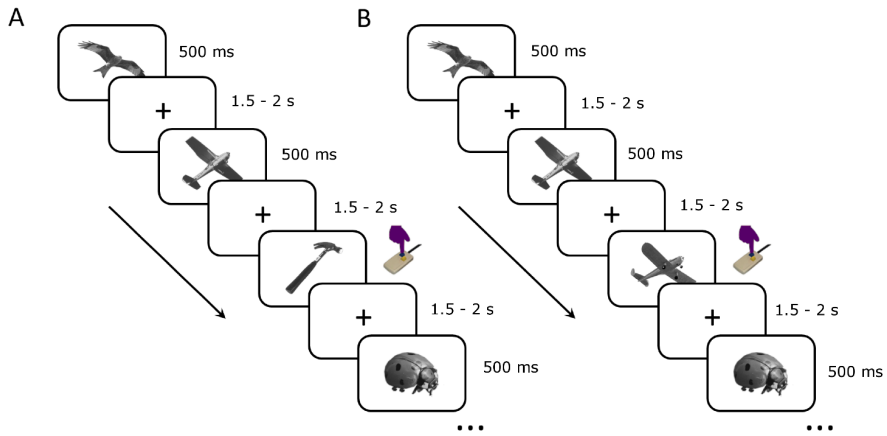

Figure 1. MEG paradigms. *(A) In Experiment 1, individual stimuli were presented centrally for 500 ms, followed by a variable ISI of 1.5 – 2 s. Participants were asked to press the response button and blink whenever they saw an oddball image (a hammer). (B) In Experiment 2, the procedure was largely identical to Experiment 1, except that participants performed a one-back task, pressing the button when two images of the same object type (e.g., two planes) appeared on two consecutive trials.*

Representational similarity analysis

In order to investigate the independent contributions of shape/texture and object category to the MEG signal, we used representational similarity analysis (RSA; Kriegeskorte et al., 2008a). Following the analysis approach used in a previous fMRI study (Proklova et al., 2016), the neural dissimilarity (measured with MEG) at each time point was modeled as a linear combination of category and perceptual dissimilarity. The procedures used to obtain the neural dissimilarity matrices as well as category and perceptual dissimilarity matrices are described below.

Category dissimilarity

A category dissimilarity matrix was constructed by assigning zeroes (minimum dissimilarity) to elements of the matrix that corresponded to pairs of objects belonging to the same category and ones (maximum dissimilarity) for pairs of objects from different categories.

Perceptual dissimilarity

Three perceptual dissimilarity matrices quantifying overall perceptual dissimilarity, outline dissimilarity, and texture dissimilarity were obtained from separate behavioral visual search experiments performed by different groups of participants (see Proklova et al., 2016 for a detailed reporting of these experiments). In each of the three experiments, participants detected an oddball target among an array of identical distractors (Figure 2B) and indicated whether the oddball was on

the right or on the left of the midline. In this task, the identity or category of the target is irrelevant; the task of the participants is simply to indicate where the different-looking stimulus is located (Mohan and Arun, 2012). This was done for all possible target-distractor pairs among the stimuli. For each pair of stimuli, the corresponding entry in the visual dissimilarity matrix is given as the inverse reaction time (1/RT) in the oddball task, using one of the stimuli as a target and another as a distractor (Figure 2C). For perceptually similar oddball and distractor pairs, the reaction times will be slower (such as when searching for a snake among ropes), while for perceptually dissimilar oddball and distractor pairs the reaction times will be faster (such as when looking for a snake among planes).

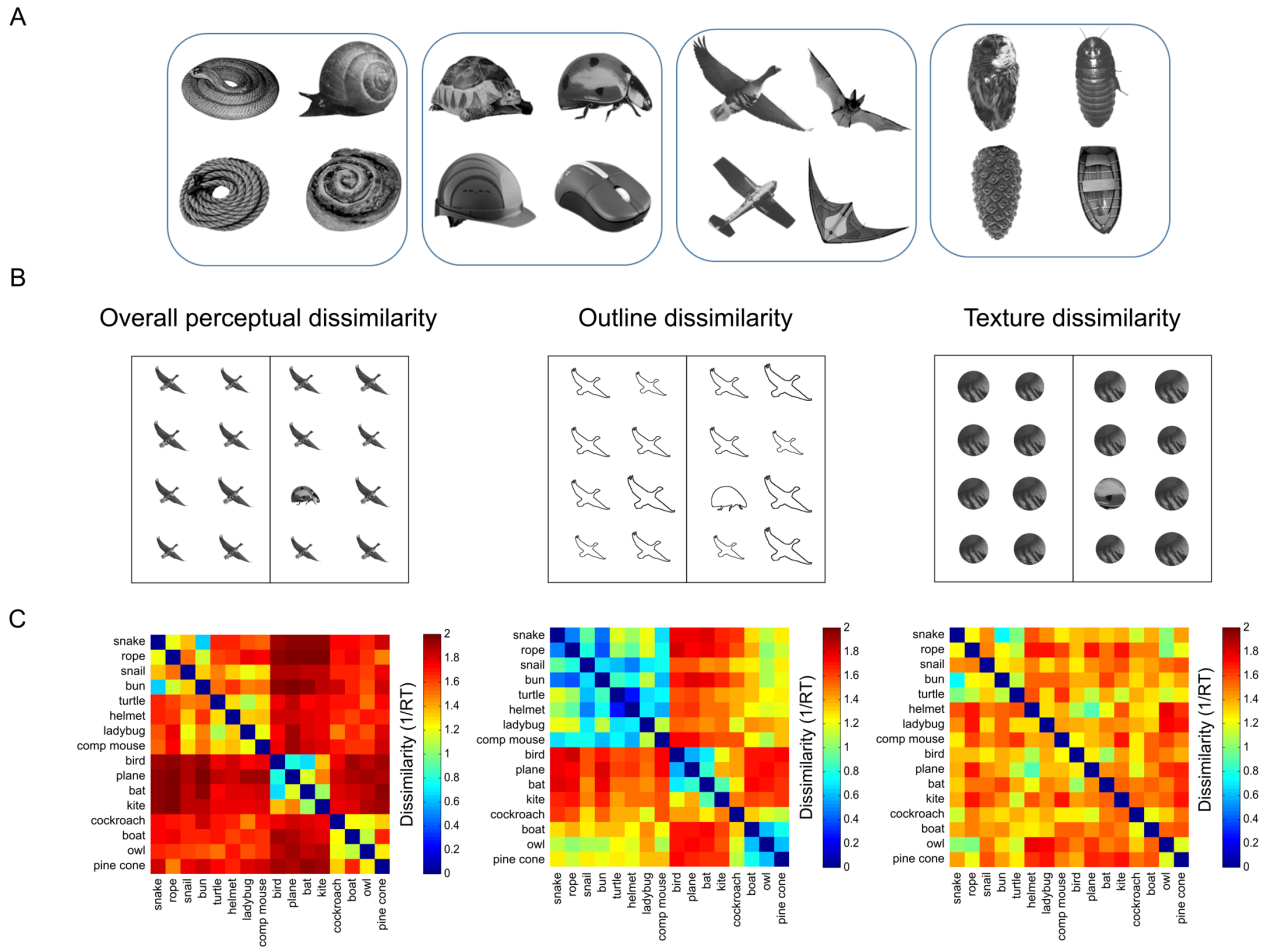

Figure 2. Stimuli and visual dissimilarity measures. *(A) The stimulus set. (B) Three behavioral visual search experiments were used to measure different aspects of pairwise perceptual dissimilarity of the stimuli. In each experiment, participants had to locate the target among the array of identical distractors. The inverse reaction time in this task is taken as a measure of perceptual dissimilarity between the target and distractor (see Proklova et al., 2016). (C) Perceptual dissimilarity matrices for the three experiments, quantifying overall perceptual dissimilarity (left panel), outline dissimilarity (center), and texture dissimilarity (right panel).*

Neural dissimilarity

Following the approach used in previous MEG decoding studies, we used pairwise decoding accuracy as a measure of neural dissimilarity, where higher decoding accuracy corresponds to greater neural dissimilarity (Cichy et al., 2014; Wardle et al., 2016). For each time point, we trained linear discriminant analysis (LDA) classifiers to discriminate between all possible pairs of stimuli. For the classification analysis, trials were randomly assigned to four independent chunks, with an equal number of trials for each condition per chunk. Classifiers were trained on data from three chunks and tested on the fourth chunk; this analysis was repeated four times, with each chunk serving as the test set once. To reduce trial-to-trial noise and increase the reliability of data supplied to the classifier, new, "synthetic" trials were created: for every condition and chunk we randomly picked 25% of the original trials and averaged the data across them. This procedure was repeated 500 times (with the constraint that no trial was used more than one time more often than any other trial), producing 500 new trials for each condition and chunk that were then supplied to the classifier. The resulting decoding accuracy time course was smoothed with an averaging filter spanning 3 time points (i.e., 30 ms). The classifier accuracy at each time point was assessed as the percentage of correctly classified trials (with chance performance being 50%) and was used as a measure of neural dissimilarity between the two conditions. This classification procedure was performed for all pairs of conditions, resulting in a 16 x 16 neural dissimilarity matrix for each time point.

In addition, as an alternative neural dissimilarity measure we used linear discriminant t-value (LD-t), a version of cross-validated Mahalanobis distance (Nili et al., 2014; Walther et al., 2016). To obtain an LD-t value for each pair of stimuli, the data was divided into two parts (training and testing set), and a LDA classifier was trained to discriminate between the two stimuli. The testing set was then projected on the discriminant dimension, and the t-value was computed describing how well the two stimuli are discriminated. This measure was calculated using the RSA toolbox (Nili et al., 2014). The 16 x 16 LD-t neural dissimilarity matrix was obtained for each time point.

After constructing neural dissimilarity matrices for each time point, as well as category and perceptual dissimilarity matrices, we performed two representational similarity analyses (RSA) to determine the contribution of category dissimilarity and different aspects of perceptual dissimilarity to the MEG signal. In the first analysis, the neural dissimilarity at each time point was modeled as a linear combination of category and overall perceptual dissimilarity (Figure 3A). This analysis was performed separately for each participant, resulting in two regression weights for each time point per participant. In the second analysis, the neural dissimilarity at each time point was modeled as a

linear combination of category, outline, and texture dissimilarity (Figure 3B). This produced three beta weights per participant for each time point. The time courses of the resulting beta estimates for each predictor were then tested against zero. Statistical significance was assessed using the threshold-free cluster enhancement procedure (TFCE) (Smith and Nichols, 2009) with default parameters, using multiple-comparison correction based on a sign-permutation test (with null distributions created from 10,000 bootstrapping iterations) as implemented in the CoSMoMVPA toolbox (Oosterhof et al., 2016). The resulting z-score time courses were thresholded at $Z > 1.64$ (i.e., $p < 0.05$, one-tailed) to reveal the time points for which the beta estimate for a given predictor was significantly above zero.

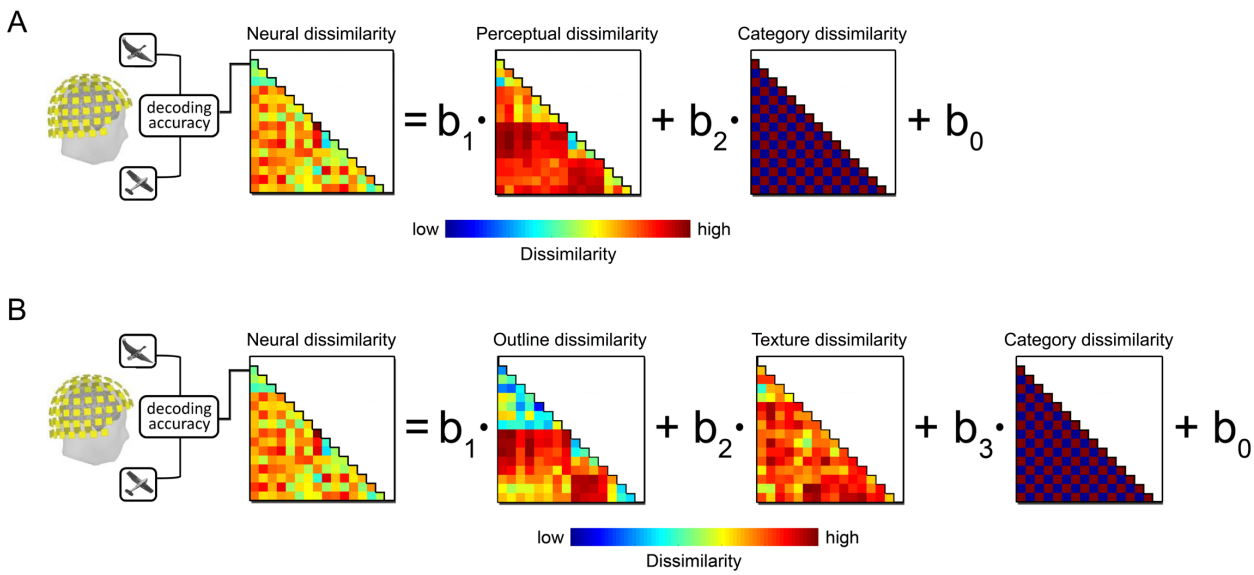

Figure 3. Representational similarity analysis. *(A) For the first RSA, at each time point, the neural dissimilarity matrix was constructed by calculating the pairwise decoding accuracy for all pairs of stimuli. This neural dissimilarity matrix was then modeled as a linear combination of overall perceptual dissimilarity and category dissimilarity. (B) For the second RSA, the neural dissimilarity at each time point was modeled using outline, texture and category dissimilarity as predictors.*

Sensor space searchlight analysis

To identify time periods and sensors in which the contribution of category or perceptual dissimilarity to neural dissimilarity was significant, we performed a sensor-space searchlight analysis. Using the same approach as in the previous analyses, we ran two representational similarity searchlights. For these analyses, the pairwise decoding analysis was repeated for local sensor neighborhoods of ten sensors each. For each sensor neighborhood the neural dissimilarity was computed for every post-

stimulus time point. Then, to reduce the number of statistical comparisons, the neural dissimilarity matrices for each neighborhood were averaged in time bins of 50 ms, ranging from stimulus onset to 500 ms post-stimulus (resulting in ten time bins).

The resulting neural dissimilarity matrices were then modeled at each time window as (1) a linear combination of category dissimilarity and overall perceptual dissimilarity, resulting in two beta estimate maps, and (2) a linear combination of category dissimilarity, outline dissimilarity, and texture dissimilarity, producing three beta estimate maps. The resulting beta estimates were mapped onto a scalp representation. The scalp maps for each predictor were then averaged across participants and tested against zero. Significance was assessed separately for each time window using the TFCE procedure (see above) to reveal the sensors in which the contribution of a particular predictor to the neural dissimilarity was significantly above chance.

Results

Behavioral results

Participants were very accurate in the oddball detection task of Experiment 1 (mean = 97%, SD = 2%) and the one-back repetition detection task of Experiment 2 (mean = 94%, SD = 1%). Responses were faster in Experiment 1 (mean = 0.47 s, SD = 0.06 s) than Experiment 2 (mean = 0.73 s, SD = 0.12 s).

Decodability of individual stimuli

To assess the quality of the MEG data and evaluate whether stimulus condition could be decoded from the MEG sensor patterns, we averaged the off-diagonal elements of the MEG dissimilarity matrix for each time point. This was done separately for Experiments 1 and 2, as well as for each of the two sensor types (magnetometers and gradiometers), producing four time courses of average pairwise stimulus decodability (Figure 4). In both experiments, and for both sensor types, decoding was at chance until about 50 ms, after which the decoding curve rose sharply, becoming significant at 60 ms (or at 70 ms for magnetometers in Experiment 2) and peaking at 120 ms. This pattern is similar to the pattern observed in previous studies (for review, see Contini et al., 2017). For both sensor types, average pairwise decoding accuracy was higher in Experiment 2, suggesting that the demands of a one-back task (e.g., enhanced attention to the objects, deeper object processing, and involvement of working memory) increases neural discriminability. Overall, these results replicate

earlier MEG decoding studies and show that the individual stimuli could be decoded successfully from the MEG signal.

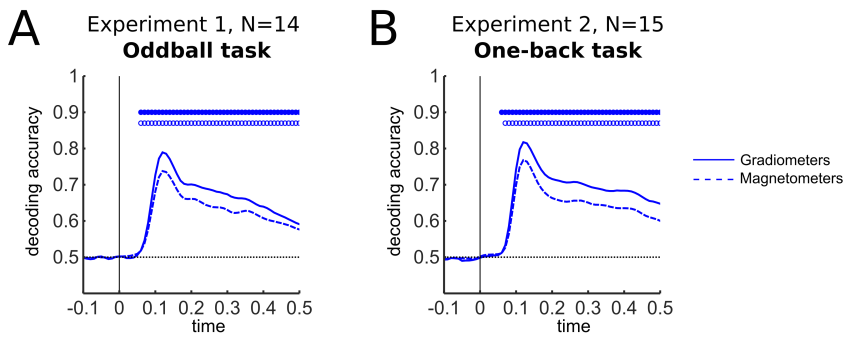

Figure 4. Time courses of average decodability of all stimulus pairs. *Average pairwise stimulus decodability in Experiment 1 (A) and Experiment 2 (B), shown separately for two sensor types (solid line for gradiometers and dashed line for magnetometers). Average pairwise decoding accuracy reaches significance at 60 ms for both types of sensors in Experiment 1 (A) and at 60 and 70 ms for gradiometers and magnetometers, respectively, in Experiment 2 (B). Average pairwise decoding accuracy peaks at 120 ms in both experiments and for both sensor types. Circles indicate time bins where decoding accuracy was significantly greater than chance (0.5), with filled circles showing significant time points for gradiometers and empty circles for magnetometers.*

Representational Similarity Analysis

To examine the contribution of overall perceptual dissimilarity and category dissimilarity to neural dissimilarity, we performed a representational similarity analysis (RSA) modelling the neural dissimilarity at each time point as the linear combination of these two predictors (see Materials and Methods; Figure 3A). This analysis produced one beta estimate time course for each predictor. The results of this analysis for both experiments (Oddball task and One-back task) are shown in Figure 5A, separately for the two types of sensors. For both magnetometers and gradiometers, the beta estimate for overall perceptual dissimilarity (shown in red) reached significance at 80 ms, peaking at 130 ms. Strikingly, the beta estimate for category dissimilarity (shown in blue) did not reach significance at any time point. In a second analysis, the neural dissimilarity was modeled as a combination of category, outline, and texture dissimilarity (Figure 3B). This analysis produced three time courses that are shown in Figure 5B. The outline predictor contributed significantly to neural dissimilarity, starting at 80 ms and peaking at 150 ms, followed by a smaller peak at 250 ms. The time course of the texture predictor was significantly above chance starting from 90 ms, with a peak at 130 ms. The beta estimate for category dissimilarity did not reach significance at any time point.

Nearly identical results were obtained in Experiment 2, in which subject performed a one-back task (Figure 5, right column). The first RSA again revealed a strong contribution of overall perceptual dissimilarity, peaking at 120 ms for magnetometers and at 130 ms for gradiometers (Figure 5A, right column). In the second RSA, the outline dissimilarity significantly contributed to the neural dissimilarity with a peak at 150 ms for both magnetometers and gradiometers (Figure 5B, right column). Texture (shown in orange) peaked at 110 ms for both types of sensors. Importantly, in both analyses the category predictor again did not reach significance at any time point, confirming the results of Experiment 1 with a different and more engaging task that required recognition of the objects.

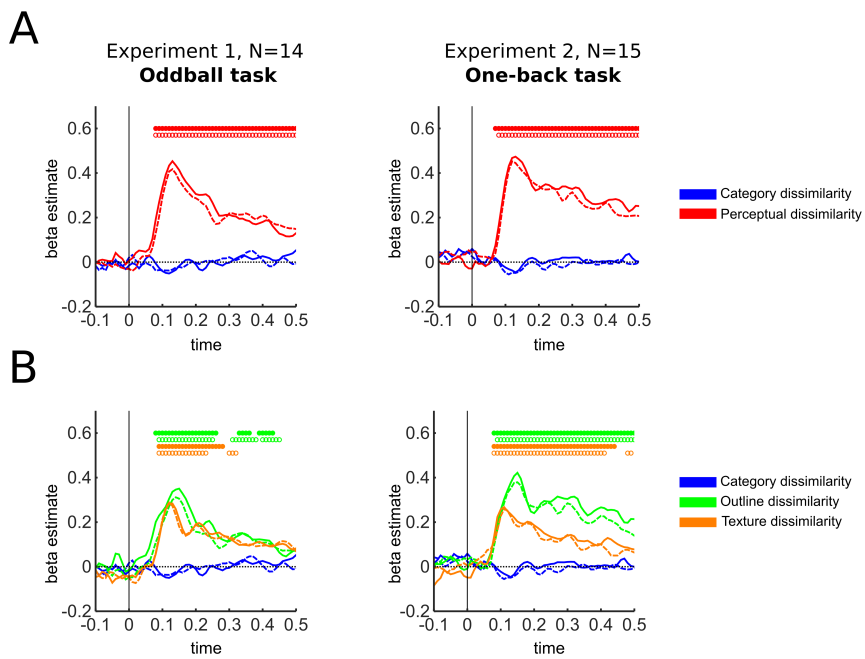

Figure 5. RSA results using decoding accuracy. *(A) The time courses of regression weights for two sensor types (solid line for gradiometers and dashed line for magnetometers) showing the contributions of category dissimilarity (in blue) and overall perceptual dissimilarity (in red) to neural dissimilarity for Experiment 1 (left column) and Experiment 2 (right column). Perceptual dissimilarity regression weights were significant starting at 80 ms, peaking at 130 ms for both magnetometers and gradiometers, while category dissimilarity was not contributing significantly to neural dissimilarity at any time point. (B) The time courses of regression weights reflecting the contributions of category dissimilarity (in blue), outline dissimilarity (in green) and texture dissimilarity (in orange). The outline dissimilarity contributed significantly to MEG signal starting at 90 ms, with a peak at 150 ms for both magnetometers and gradiometers. Texture predictor regression weights peaked at 110 ms for both types of sensors. Again, no evidence for a significant contribution of the category predictor was observed. Circles indicate time bins where beta estimates were significantly greater than zero, with filled circles showing significant time points for gradiometers and empty circles for magnetometers.*

It is possible that the previously described measure of neural dissimilarity (i.e., pairwise decoding accuracy) was not sensitive to reveal category effects. fMRI studies have suggested that the cross-validated Mahalanobis distance may be a more reliable measure of neural dissimilarity (Walther et al., 2016). Thus, we repeated all analyses using the neural dissimilarity matrices constructed using this measure (see Materials and Methods). The RSA results using this alternative neural dissimilarity measure are shown in Figure 6. The pattern of results was nearly identical to the one obtained using decoding accuracy (see Fig. 6).

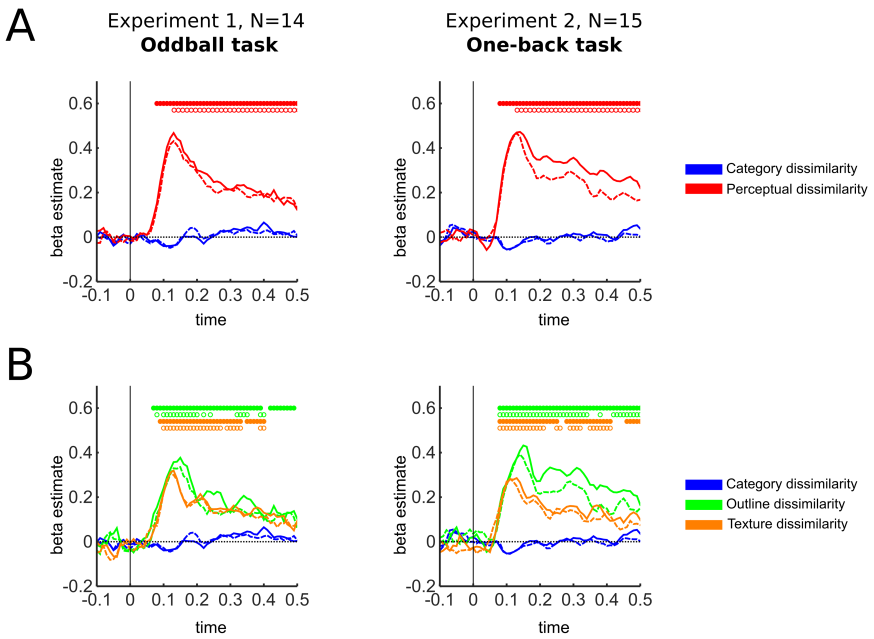

Figure 6. RSA results using cross-validated Mahalanobis distance. *(A) Contributions of category dissimilarity (in blue) and perceptual dissimilarity (in red) to neural dissimilarity for two sensor types (solid line for gradiometers and dashed line for magnetometers). Results of Experiment 1 (left column) and Experiment 2 (right column). (B) The same analysis for three predictors (outline dissimilarity, texture dissimilarity, category dissimilarity). Circles indicate time bins where beta estimates were significantly greater than zero, with filled circles showing significant time points for gradiometers and empty circles for magnetometers.*

Finally, to maximize statistical power to detect category information, we combined the data of the two experiments, resulting in N=29. Moreover, to explore the possibility that category information emerges after 500 ms, we repeated the analysis for a longer time window, until 800 ms after stimulus onset. The results of these analyses are shown in Figure 7. In the first RSA (Fig. 7A), the overall perceptual dissimilarity beta estimate peaked at 130 ms for both types of sensors and for both decoding accuracy (left column) and cross-validated Mahalanobis distance (right column) as measures of neural dissimilarity. In the second RSA (Fig. 7B), the regression weights for outline

dissimilarity peaked at 140 ms for magnetometers and at 150 ms for gradiometers for both dissimilarity measures. Texture dissimilarity beta estimates peaked at 120 ms for both sensor types. Crucially, even when combining the data from both experiments and including later time points in the analyses, no category information was found, demonstrating that MEG neural dissimilarity only reflected the perceptual dissimilarity of the objects, unlike fMRI (Proklova et al., 2016).

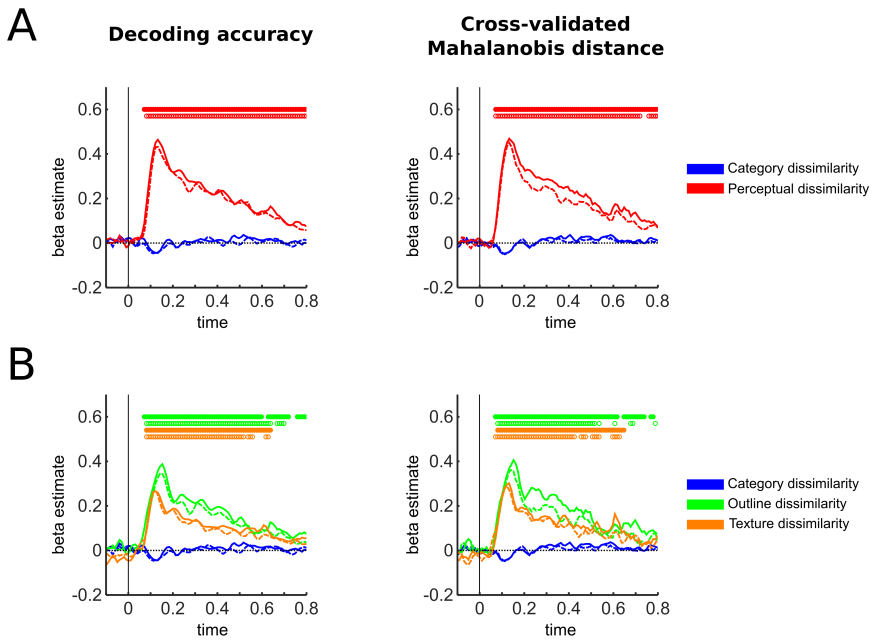

Figure 7. RSA results for both experiments combined (N=29). *(A) Contributions of category dissimilarity (in blue) and perceptual dissimilarity (in red) to neural dissimilarity for two sensor types (solid line for gradiometers and dashed line for magnetometers). Results of both experiments combined using decoding accuracy as the measure of neural dissimilarity (left column), and cross-validated Mahalanobis distance (right column). (B) The same analysis for three predictors (outline dissimilarity, texture dissimilarity, category dissimilarity). Circles indicate time bins where beta estimates were significantly greater than zero, with filled circles showing significant time points for gradiometers and empty circles for magnetometers.*

Representational Similarity Searchlight

The absence of category information in the previous analyses could in principle be due to differences in the spatial scales of visual and category processing: perhaps visual properties are well reflected in coarse patterns across all sensors, whereas more subtle categorical responses are only reflected in localized patterns emerging across a few sensors. We therefore performed a sensor-space representational similarity searchlight analysis. This analysis was done using the data from gradiometers, because these sensors showed numerically greater pairwise discriminability (see Fig. 3). Given that the pattern of results in Experiments 1 and 2 was highly similar we pooled data from Experiments 1 and 2 for the searchlight analysis to maximize power.

For each channel, we defined a neighborhood of ten adjacent channels and computed the neural dissimilarity matrix for this neighborhood (see Materials and Methods). We then used the RSA approach described earlier, modelling the neural dissimilarity for each channel as a combination of category and visual dissimilarity. This procedure was repeated for each 50 ms time window (see Materials and Methods), resulting in 10 searchlight maps showing the contribution of perceptual and category dissimilarity to neural dissimilarity at different sensor locations. In accordance with the previous analyses, this analysis did not reveal any sensors or time windows in which the contribution of category dissimilarity to neural dissimilarity was significantly above zero (Figure 8A). In contrast, the contribution of perceptual dissimilarity again reached significance in the 50-100 ms time window and stayed significant throughout all subsequent time windows, starting in a group of posterior sensors and progressing to more anterior sensors at 100-250 ms, peaking at 150-200 ms and gradually receding towards the posterior sensors again (Figure 8B). These results suggest that the MEG neural dissimilarity across multiple channel locations predominantly reflects perceptual, but not category dissimilarity, also when looking at more localized sensor patterns.

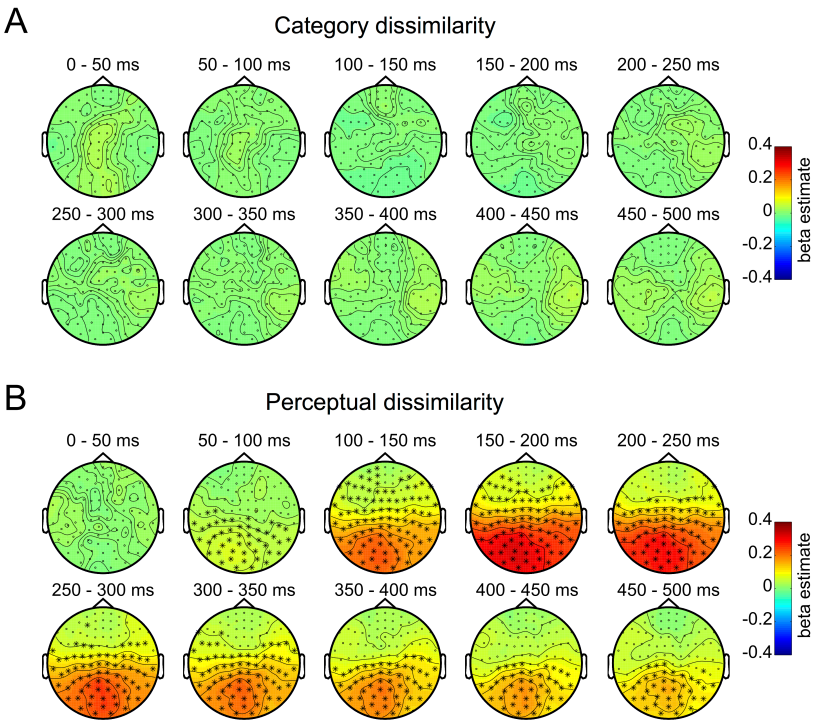

Figure 8. RSA searchlight results: category and visual perceptual dissimilarity. *(A) Searchlight maps showing the regression weights reflecting the contribution of category dissimilarity to MEG patterns across channels (gradiometers) and ten time windows. The beta estimates for category were not significantly above zero in any of the sensors for all time windows. (B) Searchlight maps showing the perceptual dissimilarity regression weights across gradiometers for ten time windows. The beta estimates are significantly above zero for a group of posterior sensors starting from 50-100 ms time window and for all the time windows after that, with activity spreading to more anterior sensors from 100 to 200*

ms but then, from around 350 ms, being again restricted to posterior sensors. The contribution of perceptual dissimilarity to the MEG signal is peaking in the 150-200 ms time window. Asterisks indicate sensor locations where beta estimates were significantly greater than zero.

Finally, we ran a second RSA searchlight, using category, outline and texture dissimilarity as predictors of neural dissimilarity. The results of this analysis are shown in Figure 9. As in the previous analysis, no sensors in any time window exhibited a significant contribution of category dissimilarity to MEG neural dissimilarity (Figure 9A). By contrast, the outline dissimilarity beta estimates reached significance at 50-100 ms after stimulus onset in a group of left posterior sensors, spreading to more anterior sensors at 100-150 ms and peaking at 150-200 ms, staying significant in posterior channels throughout all time windows (Figure 9B). Similarly, texture dissimilarity beta estimates reached significance in a cluster of central posterior sensors at 50-100 ms and stayed significant at multiple channel locations in all the next time windows, peaking at 150-200 ms (Figure 9C).

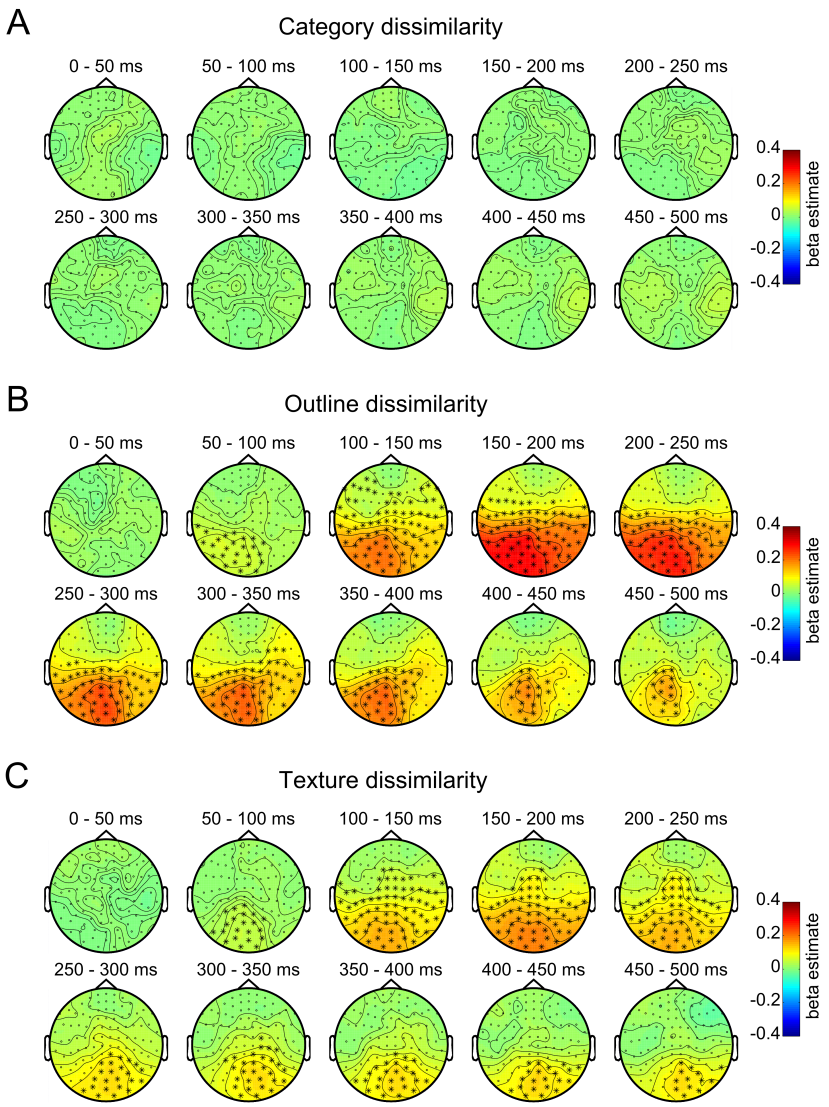

***Figure 9*. RSA searchlight results: category, outline and texture dissimilarity.** *(A) Beta estimate maps showing the contribution of category dissimilarity to MEG patterns across channels (gradiometers) and ten 50-ms time windows. The beta estimates for category did not reach significance in any of the sensors or time windows. (B) Beta estimate maps showing the contribution of outline dissimilarity to MEG signal across gradiometers for ten time windows. The beta estimates are significantly above zero for a group of posterior sensors starting from 50-100 ms time window and for all the time windows after that, with activity spreading to more anterior sensors from 100 to 200 ms, and then fading back to posterior sensors. The contribution of outline dissimilarity to MEG neural dissimilarity is peaking in the 150-200 ms time window. (C) Beta estimates reflecting contribution of texture dissimilarity to neural dissimilarity. As for the outline maps, the texture predictor reached significance in a group of posterior sensors at 50-100 ms, spreading to more anterior sensors from 100 to 250 ms with a peak at 150-200 ms and gradually receding while staying significant in posterior sensors in all the later time windows. Asterisks indicate sensor locations where beta estimates were significantly greater than zero.*

Discussion

In this study, we used a carefully selected stimulus set to disentangle perceptual from categorical factors in driving MEG sensor patterns. Replicating previous reports, MEG sensor patterns could be used to accurately decode individual objects (Carlson et al., 2011; Carlson et al., 2013; van de Nieuwenhuijzen et al., 2013; Cichy et al., 2014; Isik et al., 2014; Clarke et al., 2015; Ritchie et al., 2015; Coggan et al., 2016; Kaiser et al., 2016a). Using representational similarity analysis, we then related MEG neural similarity to the objects' perceptual and categorical similarity. This analysis revealed the time course of the objects' overall perceptual similarity as well as the separate contributions of outline shape and inner texture; each of these independently contributed to MEG neural similarity but with overlapping time courses. To our surprise, there was no category information in the MEG patterns, even though participants easily recognized the objects as being animate or inanimate (as evidenced by behavioral performance in Experiment 2).

These results can be directly compared with those of a recent fMRI study using the same stimulus set, task, and analysis approach (Proklova et al., 2016). Similar to the current MEG findings, outline shape and texture also contributed independently to multi-voxel fMRI patterns in visual cortex, with these regions partly overlapping. However, unlike the current MEG results, fMRI showed a highly reliable contribution of object category to neural similarity in anterior ventral temporal cortex. Our results therefore suggest that MEG pattern analysis simply does not have sufficient spatial resolution to discriminate between animate and inanimate neural activity patterns in ventral temporal cortex. Our results may thus point to methodological limitations of MEG pattern

analysis in relation to fMRI pattern analysis, showing that these different spatial scales reflect partly different information during object processing. Such a discrepancy between information contained in local fMRI patterns and scalp-level MEG patterns precludes the straightforward integration of fMRI and MEG pattern analysis results, for example using representational similarity analysis (Cichy et al., 2014, 2016). Future work could explore whether decoding in source-space (van de Nieuwenhuijzen et al., 2013) reduces the discrepancy.

Our results show that MEG sensor patterns in the 150-250 ms range reflect perceptual stimulus aspects, including outline shape and inner texture, derived from response times in an oddball visual search task. Previous behavioral work has shown that this perceptual similarity measure can be used to predict animate-inanimate categorization times when using stimuli that naturally confound perceptual features and category (Mohan and Arun, 2012). For example, a side-view picture of a cow is quickly categorized as animate because it is perceptually relatively similar to other animals (e.g., sheep, horse, dog) and relatively dissimilar from inanimate objects. These findings, combined with our current results, suggest that previous MEG reports of animacy decoding in the 150-250 ms range likely reflected the perceptual differences between animate and inanimate objects, rather than their category. In the current stimulus set, the perceptual similarity measure no longer reflects categorical influences (Proklova et al., 2016), allowing us to dissociate these two components and reveal that MEG sensory patterns at 150-250 ms reflect perceptual object properties rather than object categorization *per se*.

It should be noted that previous studies provided some evidence for a contribution of semantic object properties to the MEG signal even at relatively early latencies (<250 ms) (Clarke et al., 2015; Coggan et al., 2016; Kaiser et al., 2016b). These studies differed from the current study in several important ways. First, none of these studies controlled for perceptual similarity using human judgments or task performance. It is likely that the semantic factors in these studies (e.g., the property “has legs”; Clarke et al., 2015) would still express in perceptual similarity differences in tasks like the oddball visual search task used here. Second, two of these studies included human faces (Coggan et al., 2016) or bodies (Kaiser et al., 2016b). The human visual system is particularly sensitive to such stimuli (Stein et al., 2012), showing highly selective and localized face- and body-selective responses in fMRI (Kanwisher, 2010). Notably, these responses are right lateralized (Willems et al., 2010), thus resulting in distinct scalp topographies (Thierry et al., 2006) that are likely more easily decodable than the bilateral animate-inanimate organization investigated here.

To conclude, the current study shows that MEG sensor patterns are highly sensitive to two independent perceptual features (outline shape and texture) of visually presented objects, quantified using behavioral perceptual similarity measures. By contrast, MEG sensor patterns appear insensitive to the conceptual-level distinction between animate and inanimate objects, unlike fMRI voxel patterns in ventral temporal cortex (Proklova et al., 2016). This discrepancy between MEG and fMRI results should be considered in attempts to integrate these methods.

References

Amedi A, Hofstetter S, Maidenbaum S, Heimler B (2017) Task Selectivity as a Comprehensive Principle for Brain Organization. Trends Cogn Sci 21:307-310.

Bracci S, Op de Beeck H (2016) Dissociations and Associations between Shape and Category Representations in the Two Visual Pathways. J Neurosci 36:432-444.

Brainard DH (1997) The Psychophysics Toolbox. Spat Vis 10:433-436.

Bryan PB, Julian JB, Epstein RA (2016) Rectilinear Edge Selectivity Is Insufficient to Explain the Category Selectivity of the Parahippocampal Place Area. Front Hum Neurosci 10:137.

Carlson T, Tovar DA, Alink A, Kriegeskorte N (2013) Representational dynamics of object vision: the first 1000 ms. J Vis 13.

Carlson TA, Hogendoorn H, Kanai R, Mesik J, Turret J (2011) High temporal resolution decoding of object position and category. J Vis 11.

Cichy RM, Pantazis D, Oliva A (2014) Resolving human object recognition in space and time. Nat Neurosci 17:455-462.

Cichy RM, Pantazis D, Oliva A (2016) Similarity-Based Fusion of MEG and fMRI Reveals Spatio-Temporal Dynamics in Human Cortex During Visual Object Recognition. Cereb Cortex 26:3563-3579.

Clarke A, Devereux BJ, Randall B, Tyler LK (2015) Predicting the Time Course of Individual Objects with MEG. Cereb Cortex 25:3602-3612.

Coggan DD, Baker DH, Andrews TJ (2016) The Role of Visual and Semantic Properties in the Emergence of Category-Specific Patterns of Neural Response in the Human Brain. eNeuro 3.

Contini EW, Wardle SG, Carlson TA (2017) Decoding the time-course of object recognition in the human brain: From visual features to categorical decisions. Neuropsychologia 105:165-176.

Grootswagers T, Wardle SG, Carlson TA (2017) Decoding Dynamic Brain Patterns from Evoked Responses: A Tutorial on Multivariate Pattern Analysis Applied to Time Series Neuroimaging Data. J Cogn Neurosci 29:677-697.

Isik L, Meyers EM, Leibo JZ, Poggio T (2014) The dynamics of invariant object recognition in the human visual system. J Neurophysiol 111:91-102.

Kaiser D, Oosterhof NN, Peelen MV (2016a) The Neural Dynamics of Attentional Selection in Natural Scenes. J Neurosci 36:10522-10528.

Kaiser D, Azzalini DC, Peelen MV (2016b) Shape-independent object category responses revealed by MEG and fMRI decoding. J Neurophysiol 115:2246-2250.

Kanwisher N (2010) Functional specificity in the human brain: a window into the functional architecture of the mind. Proc Natl Acad Sci U S A 107:11163-11170.

Kriegeskorte N, Mur M, Bandettini P (2008a) Representational similarity analysis - connecting the branches of systems neuroscience. Front Syst Neurosci 2:4.

Kriegeskorte N, Mur M, Ruff DA, Kiani R, Bodurka J, Esteky H, Tanaka K, Bandettini PA (2008b) Matching categorical object representations in inferior temporal cortex of man and monkey. Neuron 60:1126-1141.

Macdonald SN, Culham JC (2015) Do human brain areas involved in visuomotor actions show a preference for real tools over visually similar non-tools? Neuropsychologia 77:35-41.

Mohan K, Arun SP (2012) Similarity relations in visual search predict rapid visual categorization. J Vis 12:19.

Nili H, Wingfield C, Walther A, Su L, Marslen-Wilson W, Kriegeskorte N (2014) A toolbox for representational similarity analysis. PLoS Comput Biol 10:e1003553.

Oostenveld R, Fries P, Maris E, Schoffelen JM (2011) FieldTrip: Open source software for advanced analysis of MEG, EEG, and invasive electrophysiological data. Comput Intell Neurosci 2011:156869.

Oosterhof NN, Connolly AC, Haxby JV (2016) CoSMoMVPA: Multi-Modal Multivariate Pattern Analysis of Neuroimaging Data in Matlab/GNU Octave. Front Neuroinform 10:27.

Peelen MV, Downing PE (2017) Category selectivity in human visual cortex: Beyond visual object recognition. Neuropsychologia 105:177-183.

Proklova D, Kaiser D, Peelen MV (2016) Disentangling Representations of Object Shape and Object Category in Human Visual Cortex: The Animate-Inanimate Distinction. J Cogn Neurosci 28:680-692.

Ritchie JB, Tovar DA, Carlson TA (2015) Emerging Object Representations in the Visual System Predict Reaction Times for Categorization. PLoS Comput Biol 11:e1004316.

Smith SM, Nichols TE (2009) Threshold-free cluster enhancement: addressing problems of smoothing, threshold dependence and localisation in cluster inference. Neuroimage 44:83-98.

Stein T, Sterzer P, Peelen MV (2012) Privileged detection of conspecifics: evidence from inversion effects during continuous flash suppression. Cognition 125:64-79.

Thierry G, Pegna AJ, Dodds C, Roberts M, Basan S, Downing P (2006) An event-related potential component sensitive to images of the human body. Neuroimage 32:871-879.

van de Nieuwenhuijzen ME, Backus AR, Bahramisharif A, Doeller CF, Jensen O, van Gerven MA (2013) MEG-based decoding of the spatiotemporal dynamics of visual category perception. Neuroimage 83:1063-1073.

Walther A, Nili H, Ejaz N, Alink A, Kriegeskorte N, Diedrichsen J (2016) Reliability of dissimilarity measures for multi-voxel pattern analysis. Neuroimage 137:188-200.

Wardle SG, Kriegeskorte N, Grootswagers T, Khaligh-Razavi SM, Carlson TA (2016) Perceptual similarity of visual patterns predicts dynamic neural activation patterns measured with MEG. Neuroimage 132:59-70.

Willems RM, Peelen MV, Hagoort P (2010) Cerebral lateralization of face-selective and body-selective visual areas depends on handedness. Cereb Cortex 20:1719-1725.

Willenbockel V, Sadr J, Fiset D, Horne GO, Gosselin F, Tanaka JW (2010) Controlling low-level image properties: the SHINE toolbox. Behav Res Methods 42:671-684.